Anatomical Region-Specific In Vivo Wireless Communication Channel Characterization

Ali Fatih Demir, *Student Member, IEEE*, Qammer H. Abbasi, *Senior Member, IEEE*, Z. Esat Ankarali, *Student Member, IEEE*, Akram Alomainy, *Senior Member, IEEE*, Khalid Qaraqe, *Senior Member, IEEE*, Erchin Serpedin, *Fellow, IEEE*, and Huseyin Arslan, *Fellow, IEEE*

***Abstract*— *In vivo* wireless body area networks and their associated technologies are shaping the future of healthcare by providing continuous health monitoring and noninvasive surgical capabilities, in addition to remote diagnostic and treatment of diseases. To fully exploit the potential of such devices, it is necessary to characterize the communication channel, which will help to build reliable and high-performance communication systems. This paper presents an *in vivo* wireless communication channel characterization for male torso both numerically and experimentally (on a human cadaver) considering various organs at 915 MHz and 2.4 GHz. A statistical path loss (PL) model is introduced, and the anatomical region-specific parameters are provided. It is found that the mean PL in decibel scale exhibits a linear decaying characteristic rather than an exponential decaying profile inside the body, and the power decay rate is approximately twice at 2.4 GHz as compared to 915 MHz. Moreover, the variance of shadowing increases significantly as the *in vivo* antenna is placed deeper inside the body since the main scatterers are present in the vicinity of the antenna. Multipath propagation characteristics are also investigated to facilitate proper waveform designs in the future wireless healthcare systems, and a root-mean-square delay spread of 2.76 ns is observed at 5 cm depth. Results show that the *in vivo* channel exhibit different characteristics than the classical communication channels, and location dependence is very critical for accurate, reliable, and energy-efficient link budget calculations.**

***Index Terms*—Channel characterization, implants, in/on-body communication, *in vivo*, wireless body area networks (WBANs).**

Manuscript received June 10, 2016; revised September 9, 2016; accepted October 13, 2016. Date of publication October 19, 2016; date of current version September 1, 2017. This work was supported by NPRP Grant # NPRP 6-415-3-111 from the Qatar National Research Fund (a member of Qatar Foundation).

A. F. Demir and Z. E. Ankarali are with the Department of Electrical Engineering, University of South Florida, Tampa, FL 33620 USA (e-mail: afdemir@mail.usf.edu; zekeriyya@mail.usf.edu).

Q. H. Abbasi and K. Qaraqe are with the Department of Electrical and Computer Engineering, Texas A&M University at Qatar, Doha 23874, Qatar (e-mail: qammer.abbasi@tamu.edu; k.qaraqe@tamu.edu).

E. Serpedin is with the Department of Electrical and Computer Engineering, Texas A&M University, College Station, TX 77843-1372 USA (e-mail: eserpedin@tamu.edu).

A. Alomainy is with the School of Electrical Engineering and Computer Science, Queen Mary University of London, London E1 4NS, U.K. (e-mail: a.alomainy@qmul.ac.uk).

H. Arslan is with the Department of Electrical Engineering, University of South Florida, Tampa, FL 33620 USA, and also with the College of Engineering, Istanbul Medipol University, 34083 Istanbul, Turkey (e-mail: arslan@usf.edu).

Digital Object Identifier 10.1109/JBHI.2016.2618890

I. Introduction

CHRONIC diseases and conditions such as diabetes, obesity, heart disease, and stroke are the leading causes of death and disabilities in the United States. Treating people with these illnesses accounts for 86%[1] of the national health expenditure, which is expected to be almost double in the next ten years.[2] However, these are the most preventable and manageable problems among all health issues by committing to a healthier lifestyle. Continuous health monitoring helps to achieve this goal by assisting people to engage in their healthcare and also allows physicians to perform more reliable analysis by providing the data collected over a large period of time. In addition, exploitation of this *big data* will replace the traditional "one-size-fits-all" model with more personalized healthcare in the near future. Furthermore, noninvasive surgery and remote treatment are expected to lower the risk of infection, reduce hospitalization time, and accelerate recovery processes. All these demanding requirements for an effective service quality in healthcare awakened a general interest in wireless body area networks (WBANs) research [1]–[10]. One component of such advanced technologies is represented by wireless *in vivo* sensors and actuators, e.g., pacemakers, internal drug delivery devices, nerve stimulators, and wireless capsules as shown in Fig. 1. *In vivo* medical devices offer a cost efficient and scalable solution along with the integration of wearable devices and help to achieve the vision of advanced pervasive healthcare, anytime and anywhere [1]. Besides healthcare, the use of *in vivo* WBANs is also envisioned for many other applications such as military, athletic training, physical education, entertainment, safeguarding, and consumer electronics [11], [12].

In vivo WBANs andtheir associated technologies will shape the future of healthcare considering all the potentials and the critical role of these applications. To fully exploit the use of them for practical applications, it is necessary to obtain accurate channel models that are mandatory to build reliable, efficient, and high-performance communication systems. These models are required not only to optimize the quality of service metrics such as high data rate, low bit-error rate, and latency but also to ensure the safety of biological tissues by careful link budget evaluations. Although, on-body wireless communication channel characteristics have been thoroughly investigated

[1]http://www.cdc.gov/chronicdisease

[2]https://www.cms.gov

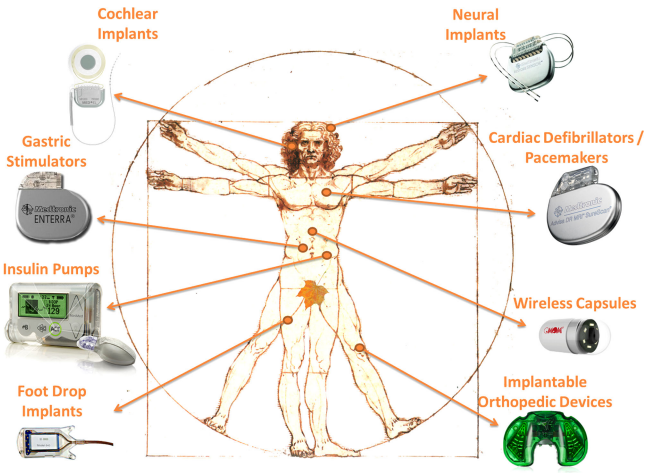

Fig. 1. *In vivo*-WBAN devices for various applications.

[3], [13], the studies on *in vivo* wireless communication channels (implant-to-implant and implant-to-external device links) are limited. The *in vivo* channel exhibits different characteristics than those of the more familiar wireless cellular and Wi-Fi environments since the electromagnetic (EM) wave propagates through a very lossy environment inside the body, and dominant scatterers are present in the near-field region of the antenna.

The IEEE 802.15.6 standard [14] was released in 2012 to regulate short-range wireless communications inside or in the vicinity of the human body. According to this standard, *in vivo*-WBAN devices operate in the medical device radio communications service (MedRadio), which uses discrete bands within the 401–457-MHz spectrum including the previous specification called medical implant communication service band. Despite the fact that MedRadio bands provide satisfying propagation characteristics inside the human body [15], they suffer from lower bandwidths and larger antenna size issues compared to the antennas designed to operate at higher frequencies. Therefore, other frequency bands, such as industrial, scientific, medical (ISM) and ultrawide band (UWB) communications bands should also be considered in the upcoming standards for *in vivo* wireless communications. It is also known that EM wave propagation inside the human body is strongly related to the location of the antenna [8], [15], and hence, the *in vivo* channel should be investigated for a specific anatomical part. For example, the gastrointestinal tract has been studied for wireless capsule endoscopy applications [16], while the heart area has been investigated for implantable cardioverter defibrillators and pacemakers [17]. Although many *in vivo* path loss (PL) formulas were reported in the literature [4]–[7], [17]–[19], they do not provide location-specific PL model parameters to carry out accurate link budget calculations. Moreover, detailed human body models are crucial in order to investigate the *in vivo* wireless communication channel. Various phantoms have been designed to simulate the dielectric properties of the tissues for numerical and experimental investigation. The validation of numerical studies with real experimental measurements is required, however performing experiments on a living human is strictly regulated. Therefore, physical phantoms [4], [8], [18] or anesthetized animals [5], [6] are often used for experimental investigations.

This paper presents a numerical and experimental characterization of the *in vivo* wireless communication channel for male torso considering various anatomical regions. The location-dependent characteristics of the *in vivo* channel are investigated by performing extensive simulations at 915 MHz and 2.4 GHz using HFSS. A statistical PL formula is introduced, and anatomical region-specific parameters are provided. The multipath propagation characteristics of the *in vivo* channel are examined by investigating the polarization and analyzing the delay spread, which is of particular importance for broadband applications. In addition to the thorough simulation studies, experiments are conducted on a human cadaver, and the results are compared with the numerical studies. The preliminary results were presented in [20] and [21]. To the best of authors' knowledge, this is the first study that investigates the *in vivo* wireless channel for various anatomical regions both numerically and experimentally on a human cadaver.

The rest of this paper is organized as follows. Section II describes the simulation/experimental setup and explains the measurement methodology in detail. Section III presents the *in vivo* channel characterization based on the numerical and experimental investigation. A statistical PL formula is provided along with the anatomical region-specific parameters, and multipath propagation characteristics are examined thoroughly. Finally, Section IV summarizes the contributions and concludes this paper.

II. Simulation and Measurement Settings

A. Simulation Setup

Analytical methods are viewed as infeasible and require extreme simplifications [2], [22]. Therefore, numerical methods, which provide less complex and appropriate approximations to Maxwell' s equations, are preferred for characterizing the *in vivo* wireless communication channel. In this study, we used ANSYS HFSS 15.0 [23], which is a full-wave EM field simulator based on the finite-element method. ANSYS also provides a detailed male human body model, and it includes frequency-dependent dielectric properties of over 300 parts (bones, tissues, and organs) with 2-mm resolution. This extensive simulation work was beyond the capability of personal computers and advanced computing resources at the University of South Florida (USF) were used to solve such large EM problems. Research Computing at USF hosts a computer cluster, which currently consists of approximately 500 nodes with nearly 7200 processors cores and 24 TB of memory in total.

The simulations were designed considering an implant to an external device (in-body to on-body) communications scenario in the male torso with a similar measurement setup in [20]. Rather than using the whole body, the torso area was segmented into four sectors considering the major internal organs: heart, stomach, kidneys, and intestine as shown in Fig. 2(a). In each region, simulations were performed by rotating receiver (*ex vivo*) and transmitter (*in vivo*) antennas together around the body with 22.5° angle increments [see Fig. 2(b)]. The *ex vivo* antenna was

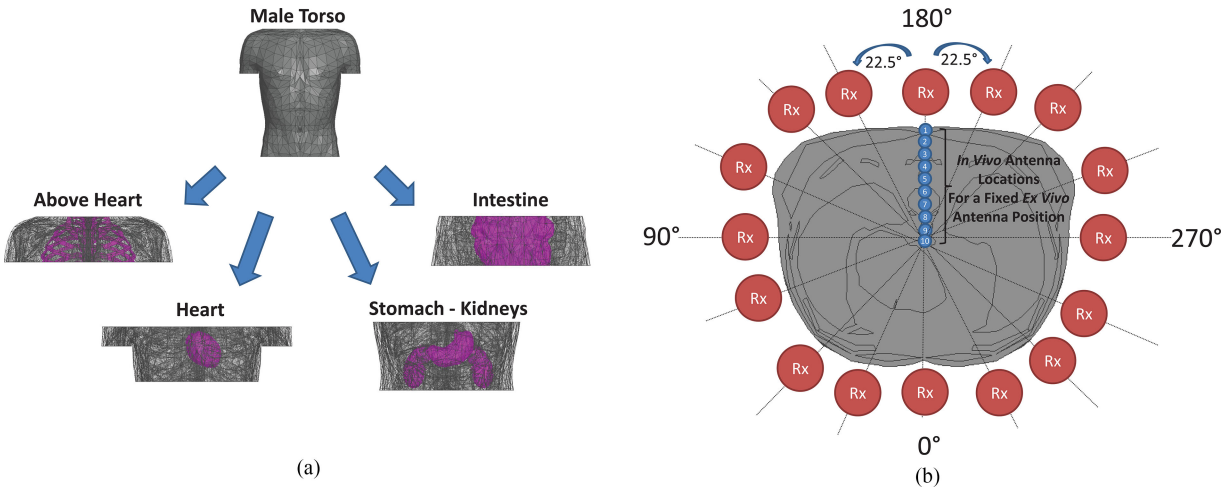

Fig. 2. (a) Investigated anatomical regions. (b) *In vivo* and *ex vivo* antenna locations in simulations. 16 (angles) × 10 (depth) × 4 (regions) × 2 (operational frequencies) = 1280 simulations were performed in total for the PL model.

placed 5 cm away from the body surface and the *in vivo* antenna was placed at ten different depths (from 10 to 100 mm) inside the body for each *ex vivo* antenna location. In addition, antennas were placed in the same orientation to avoid polarization losses.

The received power is expressed using the Friss equation (1) for free space links [24].

$$P_r = P_t G_t \left(1 - |S_{11}|^2\right) G_r \left(1 - |S_{22}|^2\right) \left(\frac{\lambda}{4\pi R}\right)^2 \quad (1)$$

where P_t/P_r represents transmitted/received powers, G_t/G_r denotes the gain of the transmitter/receiver antenna, λ stands for the free space wavelength, R is the distance between transmitter and receiver antennas, and $|S_{11}|$, $|S_{22}|$ are the reflection coefficients of transmitter/receiver antennas. Unlike free-space communications, *in vivo* antennas are often considered to be an integral part of the channel [2] (i.e., the gain cannot be separated from the channel), and hence, they need to be designed carefully. However, omnidirectional dipole antennas at 915 MHz and 2.4 GHz were deployed in our simulations for simplicity. The dipole antenna length is proportional to the wavelength, which varies with respect to both frequency and permittivity. Higher frequencies compared to the MedRadio bands provide smaller antenna sizes, hence, they could be implanted conveniently. In addition, the antennas were optimized inside the body with respect to the average torso permittivity for each frequency toward obtaining maximum power delivery. Although the antennas presented a good return loss (i.e., less than -7 dB), they were perfectly matched by compensating the $(1 - |S_{11}|^2)$ and $(1 - |S_{22}|^2)$ factors to yield a fair comparison for PL analysis. Also, the mesh size was set to be less than $\lambda/5$ in this study.

B. Experimental Setup

The numerical investigation was validated by conducting experiments on a human cadaver in a laboratory environment. Istanbul Medipol University provided the ethical approval and medical assistance in this study. The preliminary results were presented in [21]. Animal organs are used to represent human tissues as suggested in [18], [25], and [26], and the decayed human internal organs in this experiment were replaced with internal organs of a sheep. The male torso area was investigated at 915 MHz by measuring the channel frequency response, i.e., $S_{21}(f)$, through a vector network analyzer (VNA). A tapered slot coplanar waveguide (CPW)-fed antenna [27] (*in vivo*) and a dipole antenna (*ex vivo*) were used in our experiments with two coaxial cables each having a length of 2 m as illustrated in Fig. 3. The frequency response of cables was subtracted from the channel measurements by performing a calibration of the VNA. The antennas were wrapped with a biocompatible polyethylene protective layer and sealed tightly in order not to contact the biological tissues directly, which could lead to shortening the antennas. The antennas were tested before the experiment and provided sufficient return loss inside the body during the experiments (i.e., less than -7 dB).

Fig. 3. Experiment setup for *the in vivo* channel: 1) VNA, 2) human male cadaver, 3) coaxial cables, 4) a novel tapered slot CPW-fed antenna (*in vivo*), and 5) insulated dipole antenna (*ex vivo*).

The *in vivo* antenna was placed at six different locations (see Fig. 4) inside the body around the heart, stomach, and intestine by the help of a physician. *In vivo* depth measurements were performed using a digital caliper and the antennas were placed with the same orientation to avoid polarization losses, similar to the simulations. The channel data were captured

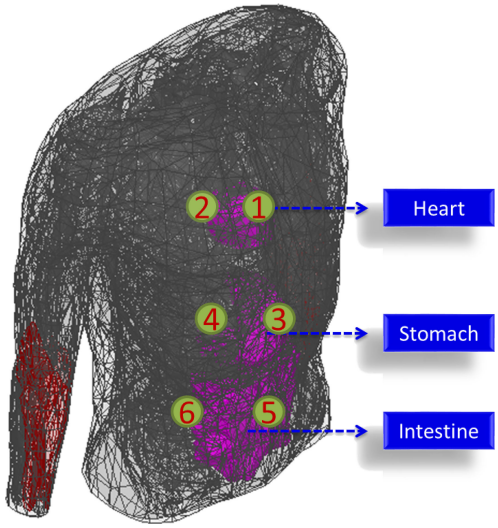

Fig. 4. Measurement locations on the human cadaver, where odd and even numbers represent top and bottom of the corresponding organs, respectively.

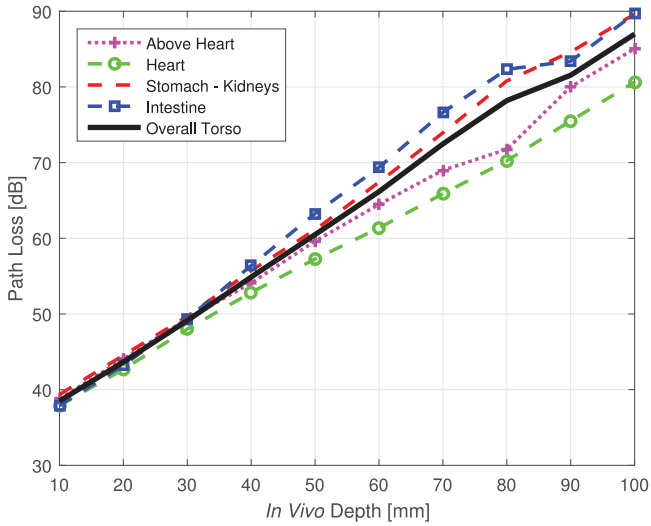

Fig. 5. Average PL for four anatomical regions in the simulation environment at 2.4 GHz.

between the frequencies 905 and 925 MHz and postprocessed for further analysis in MATLAB. Although the experimental setup did not allow capturing the effects of circulatory and respiratory systems, it provides a more realistic multipath propagation scenario than computer simulations or experiments, which are conducted on physical phantoms and anesthetized animals by providing EM wave propagation in an actual human body.

III. *IN VIVO* Channel Characterization

A. PL and Shadowing

The *in vivo* PL expresses a measure of the average signal power attenuation inside the body and is calculated as $PL = -\text{mean}\{|S_{21}|\}$ using the channel frequency response, i.e., S_{21} [4], [5]. The location-dependent characteristic of the *in vivo* PL was investigated for two ISM bands, i.e., 915 MHz and 2.4 GHz. The EM wave propagates through various organs and tissues regarding different antenna locations, and the PL changes significantly even for equal *in vivo* depths. The location-dependent characteristic of the channel is more dominant when the *in vivo* antenna is placed deeper inside the body. Fig. 5 presents the mean PL for the investigated four anatomical body regions in the simulation environment. Although the signal power attenuation is similar for near-surface locations, complex body areas such as intestine cause higher PL due to their dense structure beyond 30 mm *in vivo* depth.

Various analytical and statistical PL formulas have been proposed for the *in vivo* channel [1]. Despite the fact that analytical expressions provide intuition about each component of the propagation models, they are not practical for link budget design. According to the final report of the IEEE 802.15.6 standard' s channel modeling subgroup, the Friis transmission equation (1) can be used for *in vivo* scenarios by adding a random variation term [28], [29]. In this paper, the *in vivo* PL is modeled statistically as a function of depth by the following equation expressed

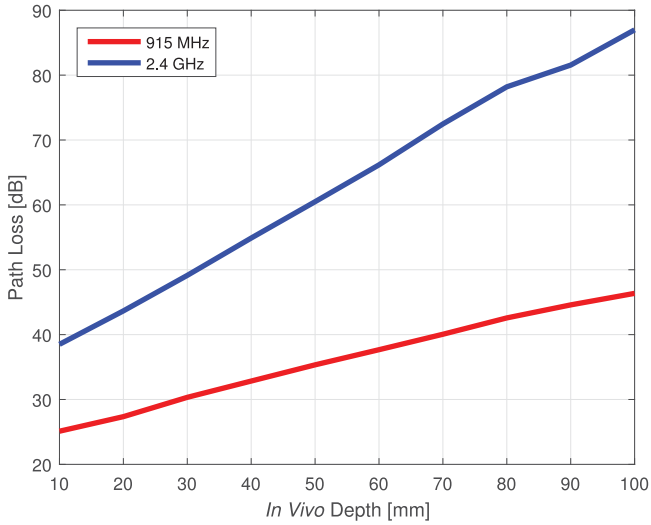

Fig. 6. Average PL on torso in the simulation environment at 915 MHz and 2.4 GHz.

in decibel scale:

$$\text{PL}(d) = \text{PL}_0 + m(d/d_0) + S \qquad (d_o \leq d) \qquad (2)$$

where d represents the depth from the body surface in mm, d_0 stands for the reference depth with a value of 10 mm, PL_0 denotes the intercept term in decibel, m is the decay rate of the received power, and S denotes the random shadowing in decibel, which presents a normal distribution for a fixed distance. The power decay rate (m) heavily depends on the environment and is obtained by performing extensive simulations and measurements. Also, the shadowing term (S) depends on the different body materials (e.g., bone, muscle, fat, etc.) and the antenna gain in different directions [17]. The proposed *in vivo* PL model is valid for $10 \leq d \leq 100$ mm and the communication channel between an *in vivo* medical device, and a far external node could

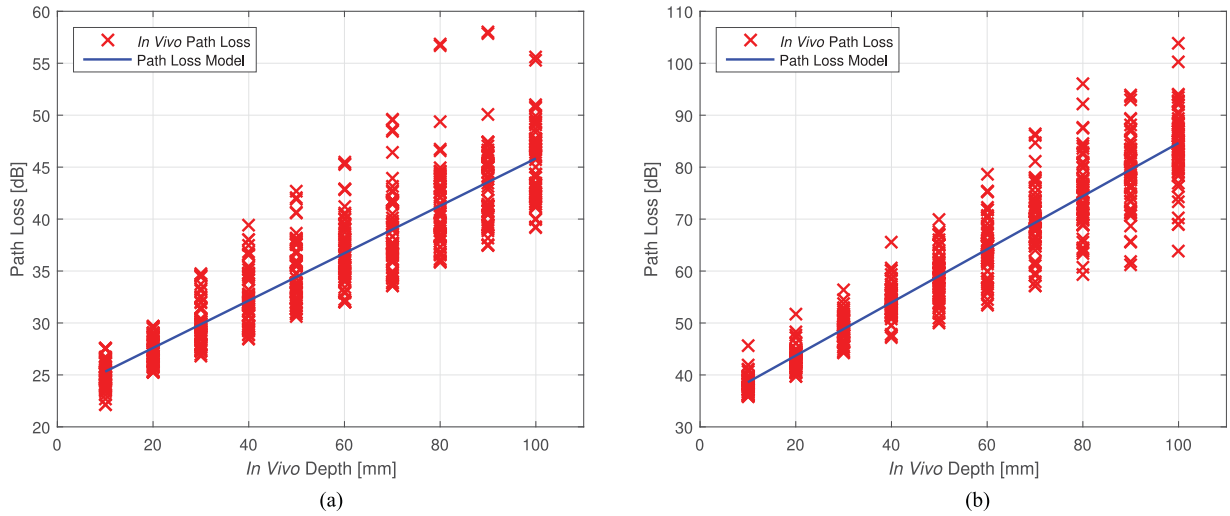

Fig. 7. Scatter plots of PL versus *in vivo* depth in the simulation environment at: (a) 915 MHz; (b) 2.4 GHz.

TABLE I
VARIANCE OF SHADOWING TERM (S) IN DECIBEL FOR EACH IN VIVO DEPTH

Frequency \ Depth	10 mm	20 mm	30 mm	40 mm	50 mm	60 mm	70 mm	80 mm	90 mm	100 mm
915 MHz	1.26	1.29	2.17	2.67	3.01	3.38	3.86	4.22	4.05	3.60
2.4 GHz	1.67	2.03	2.54	3.29	4.47	5.39	6.44	7.28	6.85	7.01

be considered as a combination of two concatenated channels: "in-body to on-body" and "classical indoor channel," if there are no surrounding objects around the body [28]. It should be pointed out that the model is antenna dependent as the majority of other WBAN propagation models in the literature, and this phenomenon is needed to be taken into account for link budget calculations as well.

Fig. 7 shows the scatter plots of PL versus *in vivo* depth on torso in the simulation environment at 915 MHz and 2.4 GHz. The mean PL is obtained using a linear regression model. It is observed that the power decay rate (m) is approximately twice at 2.4 GHz due to the high absorption in tissues as compared to 915 MHz (see Fig. 6). In addition, the variance of the shadowing term, σ, becomes notably larger as the *in vivo* antenna is placed deeper inside the body as shown in Table I. This behavior can be interpreted using the fundamental statistics theorem, which states that the variance of independent random variables' sum equals to the sum of the variances of the random variables (scattering objects) involved in the sum. The *in vivo* channel exhibits a different characteristic than the classical channels, due to the main scatterers present in the vicinity of the antenna, and the variance of shadowing increases significantly compared to free space communications.

The statistical *in vivo* PL model parameters in (2) are provided for each anatomical regions in Tables II and III, which were obtained by performing extensive simulations. By interpreting them, it could be concluded that PL increases when the *in vivo* antenna is placed in an anatomically complex region. For example, the intestine has a complex structure with repetitive, curvy-shaped, dissimilar tissue layers, while the stomach exhibits a smoother structure. As a result, the PL is greater in the intestine than in the stomach even at equal *in vivo* antenna depths. Also, more radiation occurs in the posterior region

TABLE II
STATISTICAL PL MODEL PARAMETERS (ANATOMICAL REGION)

Body Area \ Parameters	915 MHz			2.4 GHz		
	PL_0[dB]	m	σ	PL_0[dB]	m	σ
Above Heart	24.26	2.35	3.47	34.14	4.90	3.17
Heart	22.73	2.00	2.13	34.11	4.30	4.85
Stomach - Kidneys	21.90	2.51	1.68	33.03	5.54	4.08
Intestine	23.24	2.27	3.48	32.74	5.71	4.20
Overall Torso Area	23.04	2.28	3.10	33.49	5.12	5.09

TABLE III
STATISTICAL PL MODEL PARAMETERS (ANATOMICAL DIRECTION)

Body Area \ Parameters	915 MHz			2.4 GHz		
	PL_0[dB]	m	σ	PL_0[dB]	m	σ
Anterior	23.47	2.41	3.12	33.83	5.24	5.06
Posterior	23.36	2.18	1.78	33.61	5.27	3.76
Left Lateral	22.64	2.32	3.44	33.42	5.00	5.61
Right Lateral	22.54	2.32	3.29	33.17	4.94	4.99
Overall Torso Area	23.04	2.28	3.10	33.49	5.12	5.09

TABLE IV
EXPERIMENTAL PL VALUES FOR SELECTED IN VIVO LOCATIONS

Location	*In Vivo* Depth	PL
01) Above heart	3 cm	45.32 dB
02) Below heart	8 cm	55.61 dB
03) Above stomach	5 cm	48.19 dB
04) Below stomach	9 cm	50.80 dB
05) Above intestine	2 cm	29.95 dB
06) Below intestine	10 cm	50.47 dB

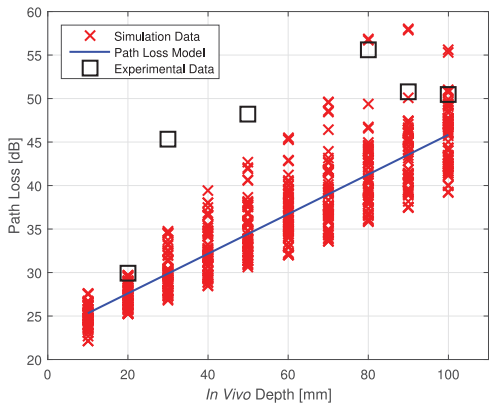

Fig. 8. PL versus *in vivo* depth from the body surface at 915 MHz.

TABLE V
COMPARISON OF THE STATISTICAL PL MODEL PARAMETERS

Environment	PL_0 [dB]	m	σ
Simulation	23.04	2.28	3.10
Experimental	33.81	2.09	5.56

than in the anterior region due to the human body structure. To sum up, the location dependence is very critical for link budget calculations and the target anatomical region should be taken into account to design a high-performance, energy-efficient communications system inside the body.

The numerical studies were validated with experiments on a human cadaver at 915 MHz. The *in vivo* antennas were placed at six different locations as shown in Fig. 4 and the *ex vivo* antenna was placed 2 cm away from the body surface. Table IV presents the PL values for the selected *in vivo* locations and comparison of experimental results with numerical studies are provided in Fig. 8. The discrepancies between the simulated and measured results exist due to the additional losses (e.g., antenna distortion), which were not considered in the simulations and the differences in experimental environment. The statistical *in vivo* PL model parameters are also provided for the experimental study and compared with the numerical study in Table V.

B. Multipath Characteristics

In addition to the PL and shadowing, multipath propagation characteristics of the *in vivo* channel are also important and should be investigated to discuss proper waveform designs.

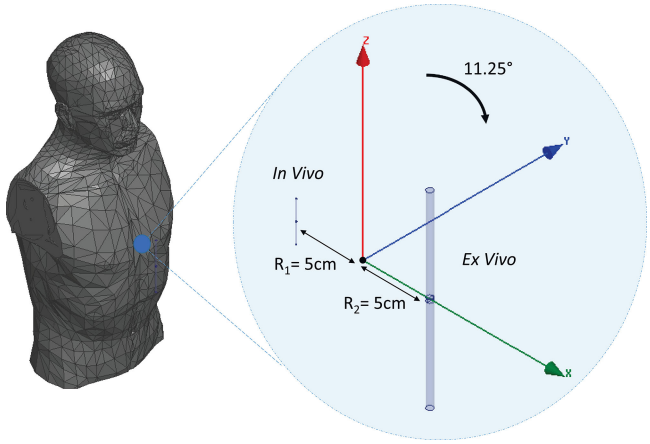

Fig. 9. Simulation setup for the *in vivo* polarization investigation.

Received signal strength was explored for various antenna polarizations toward understanding the existence of multipath reflections in the human body medium. As similar to the previous part, the dipole antennas at 915 MHz were deployed in the simulation environment, and they were perfectly matched as mentioned in Section II. The *in vivo* antenna was placed at 5 cm depth on the chest, and the *ex vivo* antenna was placed 5 cm away from the body surface to investigate the "in-body to off-body" link. As a baseline to compare with the *in vivo* channel, the antennas were separated from each other by 10 cm in free space. The *ex vivo* antenna was rotated with 11.25° increments in the YZ-plane for both scenarios as shown in Fig. 9 and the maximum available power at the receiver for different polarization mismatch angles is presented in Fig. 10. In the free space link, the received power degrades dramatically as the polarization mismatch increases due to the absence of multipath components, i.e., only line-of-sight components are effective on the received signal strength. On the other hand, the received signal power does not change significantly with polarization mismatch for *in vivo* medium. Therefore, it can be concluded that biological tissues inside the human body do not absorb the EM waves completely at 915 MHz and allow reflections that lead to multipath propagation. These reflections will cause small-scale fading, which is defined as variations over short distances due to constructive and destructive additions of the signals.

As a result of multipath propagation inside the human body, the amount of delay spread should be understood to design an efficient *in vivo* communications systems. Therefore, power delay profiles (PDPs) for various anatomical regions were extracted from the simulation results. The *in vivo* antennas were placed at 5 cm depth on the torso, and the *ex vivo* antennas were placed 5 cm away from the body surface as shown in Fig. 11 for four different directions at 915 MHz. The channel impulse response, $h(t)$, was obtained by taking the inverse discrete Fourier transform (IDFT) of the channel frequency response, S_{21}. The PDP was calculated as $\mathrm{PDP}(t) = |h(t)|^2$ and the total power is normalized to 1 as presented in Fig. 12. Related multipath channel statistics,*mean excess delay*($\overline{\tau}$), and *root-mean-square (RMS) delay spread* (σ_τ) are calculated to quantify the time-dispersion

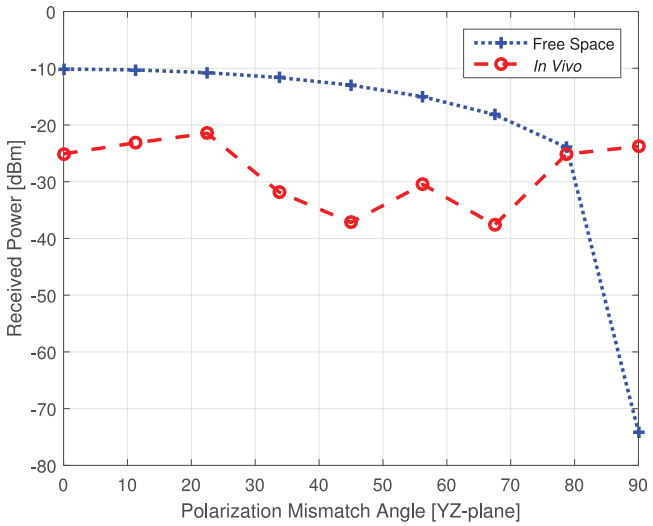

Fig. 10. Received power for various polarization mismatch angles in the simulation environment at 915 MHz.

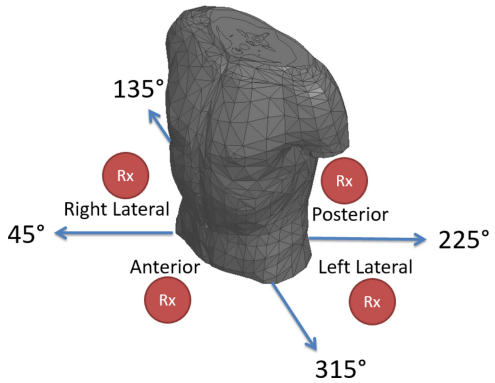

Fig. 11. Simulation setup for the *in vivo* delay spread investigation.

effect of the *in vivo* channel as follows [30]:

$$\overline{\tau} = \frac{\sum_i \tau_i P(\tau_i)}{\sum_i P(\tau_i)} \tag{3}$$

$$\sigma_\tau = \sqrt{\overline{\tau^2} - (\overline{\tau})^2} = \sqrt{\frac{\sum_i \tau_i^2 P(\tau_i)}{\sum_i P(\tau_i)} - \left(\frac{\sum_i \tau_i P(\tau_i)}{\sum_i P(\tau_i)}\right)^2} \tag{4}$$

where $P(\cdot)$ represents the received power in linear scale and, τ_i denotes the arrival time of the ith path. These parameters for various anatomical directions are listed in Table VI and it is observed that the maximum difference in σ_τ is 0.3 ns. Therefore, it can be stated that there is almost no difference in delay spread for various locations when the antennas are implanted with 5 cm depth on the torso.

RMS delay spread determines the coherence bandwidth (B_c) of the channel. It is a statistical measure of the range of frequencies where the channel can be assumed as "flat" [24] and the 90% B_c is estimated as follows:

$$B_c \approx \frac{1}{50\sigma_\tau}. \tag{5}$$

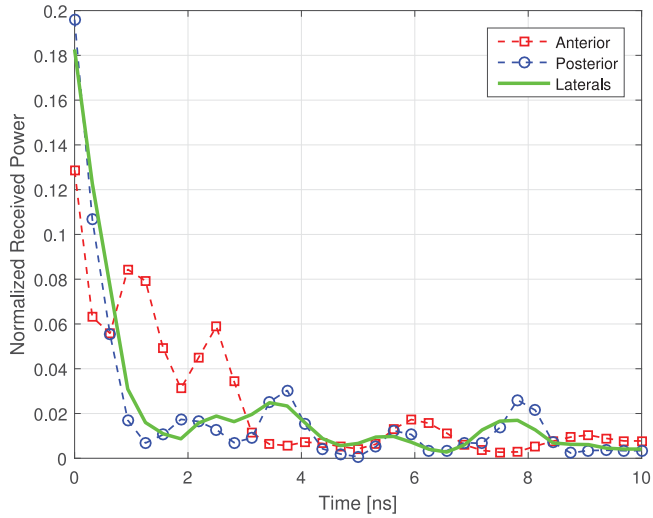

Fig. 12. Power delay profiles for each anatomical direction in the simulation environment at 915 MHz.

TABLE VI
IN VIVO MULTIPATH PROPAGATION STATISTICS AT 915 MHZ

Parameters / Body Area	Mean Excess Delay ($\overline{\tau}$) [ns]	RMS Delay Spread (σ_τ) [ns]
Anterior	2.34	2.59
Posterior	2.32	2.89
Laterals	2.27	2.79

The average σ_τ at 5 cm *in vivo* depth is measured as 2.76 ns on the torso and 7.25-MHz coherence bandwidth was predicted using (5). Theoretically, intersymbol interference (ISI) is not a critical problem when the signal bandwidth (BW) is less than B_c. Hence, the measured delay spread should not cause serious ISI for narrow-band (NB) communications. However, this dispersion may lead to a significant interference for UWB communications, which occupies a BW of greater than 500 MHz.

In frequency-selective channels (i.e., the signal BW is greater than B_c) single-carrier waveforms might not exhibit a sufficient bit error rate (BER) performance without deploying complex equalizers to solve the ISI problem. Nevertheless, power limitation is a major constraint for *in vivo*-WBAN devices, and hence, the complexity of signal processing operations must be low. Multicarrier systems are offered to provide a trivial solution for the ISI problem. For example, orthogonal frequency division multiplexing (OFDM)-based waveforms can easily handle delay spread using a cyclic prefix. However, high peak-to-average-power ratio (PAPR) emerges as a common problem in multicarrier waveforms, and it makes the signal vulnerable against the nonlinear characteristics of the radio frequency (RF) front-end components. Since the *in vivo*-WBAN devices are restricted in size, the use of high-quality components with high dynamic ranges is impractical. Therefore, PAPR remains as an important issue and may still lead the designers to use single-carrier signaling techniques. To sum up, there are tradeoffs in waveform selection considering the dispersive

nature of the *in vivo* channel and practical issues together. The system requirements in terms of throughput, power efficiency, and signal quality need to be clearly identified, and the most proper waveform technology should be selected accordingly.

IV. Conclusion

This paper presented the location-dependent characteristics of the *in vivo* wireless communications channel for male torso at 915 MHz and 2.4 GHz. Extensive simulations were performed using a detailed 3-D human body model and measurements were conducted on a human cadaver. A statistical *in vivo* PL model is introduced along with the anatomical region-specific parameters. It is observed that the PL in decibel scale follows a linear decaying profile instead of an exponential characteristic, and the power decay rate is approximately twice at 2.4 GHz as compared to 915 MHz. In addition, the variance of shadowing increases significantly as the *in vivo* antenna is placed deeper inside the body since the main scatterers are present in the vicinity of the antenna. Results show that the location dependence is very critical for link budget calculations, and the target anatomical region should be taken into account to design a high-performance *in vivo* communications system without harming the biological tissues. Multipath propagation characteristics are examined as well to facilitate proper waveforms inside the body by investigating various antenna polarizations and PDPs. A mean RMS delay spread of 2.76 ns is observed at 5 cm *in vivo* depth. Despite the fact that this dispersion may not cause significant ISI for NB communications, it could be a serious issue for UWB communications. The interest in WBANs is rapidly growing and *in vivo* medical devices are shaping the future of healthcare. This study will contribute significantly to the upcoming WBAN standards, and hence, will lead to the design of better *in vivo* transmitter/receiver algorithms.

Acknowledgment

The authors would like to thank Istanbul Medipol University, School of Medicine for providing the human cadaver and their valuable medical assistance.

References

[1] A. F. Demir *et al.*, "In vivo communications: Steps toward the next generation of implantable devices," *IEEE Veh. Technol. Mag.*, vol. 11, no. 2, pp. 32–42, Jun. 2016.

[2] P. S. Hall and Y. Hao, *Antennas and Propagation for Body-Centric Wireless Communications*, 2nd ed. Norwood, MA, USA: Artech House, 2012.

[3] Q. H. Abbasi, A. Sani, A. Alomainy, and Y. Hao, "On-body radio channel characterization and system-level modeling for multiband OFDM ultra-wideband body-centric wireless network," *IEEE Trans. Microw. Theory Techn.*, vol. 58, no. 12, pp. 3485–3492, Dec. 2010.

[4] R. Chávez-Santiago *et al.*, "Experimental path loss models for in-body communications within 2.36-2.5 GHz," *IEEE J. Biomed. Health Informat.*, vol. 19, no. 3, pp. 930–937, May 2015.

[5] P. A. Floor *et al.*, "In-body to on-body ultrawideband propagation model derived from measurements in living animals," *IEEE J. Biomed. Health Informat.*, vol. 19, no. 3, pp. 938–948, May 2015.

[6] D. Anzai *et al.*, "Experimental evaluation of implant UWB-IR transmission with living animal for body area networks," *IEEE Trans. Microw. Theory Techn.*, vol. 62, no. 1, pp. 183–192, Jan. 2014.

[7] D. Kurup, W. Joseph, G. Vermeeren, and L. Martens, "In-body path loss model for homogeneous human tissues," *IEEE Trans. Electromagn. Compat.*, vol. 54, no. 3, pp. 556–564, Jun. 2012.

[8] H. Y. Lin, M. Takahashi, K. Saito, and K. Ito, "Characteristics of electric field and radiation pattern on different locations of the human body for in-body wireless communication," *IEEE Trans. Antennas Propag.*, vol. 61, no. 10, pp. 5350–5354, Oct. 2013.

[9] A. F. Demir, H. Arslan, and I. Uysal, "Bio-inspired filter banks for SSVEP-based brain-computer interfaces," in *Proc. 2016 IEEE-EMBS Int. Conf. Biomed. Health Informat.*, Feb. 2016, pp. 144–147.

[10] A. F. Demir *et al.*, "In vivo wireless channel modeling," in *Advances in Body-Centric Wireless Communication: Applications and State-of-the-Art*. Inst. Eng. Technol., (IET) Jun. 2016, ch. 7, pp. 187–211.

[11] H. Cao, V. Leung, C. Chow, and H. Chan, "Enabling technologies for wireless body area networks: A survey and outlook," *IEEE Commun. Mag.*, vol. 47, no. 12, pp. 84–93, Dec. 2009.

[12] S. Movassaghi, M. Abolhasan, J. Lipman, D. Smith, and A. Jamalipour, "Wireless body area networks: A survey," *IEEE Commun. Surveys Tuts.*, vol. 16, no. 3, pp. 1658–1686, Third Quarter 2014.

[13] D. B. Smith, D. Miniutti, T. A. Lamahewa, and L. W. Hanlen, "Propagation models for body-area networks: A survey and new outlook," *IEEE Antennas Propag. Mag.*, vol. 55, no. 5, pp. 97–117, Oct. 2013.

[14] *IEEE Standard for Local and metropolitan area networks—Part 15.6: Wireless Body Area Networks*, IEEE Std 802.15.6-2012, pp. 1–271, Feb. 2012.

[15] A. Sani, A. Alomainy, and Y. Hao, "Numerical characterization and link budget evaluation of wireless implants considering different digital human phantoms," *IEEE Trans. Microw. Theory Techn.*, vol. 57, no. 10, pp. 2605–2613, Oct. 2009.

[16] M. R. Basar *et al.*, "The use Of a human body model to determine the variation of path losses in the human body channel in wireless capsule endoscopy," *Progress Electromagn. Res.*, vol. 133, pp. 495–513, 2013.

[17] K. Sayrafian-Pour *et al.*, "Channel models for medical implant communication," *Int. J. Wireless Inf. Netw.*, vol. 17, no. 3-4, pp. 105–112, Dec. 2010.

[18] A. Alomainy and Y. Hao, "Modeling and characterization of biotelemetric radio channel from ingested implants considering organ contents," *IEEE Trans. Antennas Propag.*, vol. 57, no. 4, pp. 999–1005, Apr. 2009.

[19] A. Khaleghi, R. Chavez-Santiago, and I. Balasingham, "Ultra-wideband statistical propagation channel model for implant sensors in the human chest," *IET Microw. Antennas Propag.*, vol. 5, no. 15, pp. 1805–1812, Dec. 2011.

[20] A. F. Demir, Q. H. Abbasi, Z. E. Ankarali, E. Serpedin, and H. Arslan, "Numerical characterization of in vivo wireless communication channels," in *Proc. 2014 IEEE MTT-S Int. Microw. Workshop Series RF Wireless Technol. Biomed. Healthcare Appl.*, Dec. 2014, pp. 1–3.

[21] A. F. Demir *et al.*, "Experimental characterization of in vivo wireless communication channels," in *Proc. 2015 IEEE 82nd Veh. Technol. Conf.*, Sep. 2015, pp. 1–2.

[22] A. Pellegrini *et al.*, "Antennas and propagation for body-centric wireless communications at millimeter-wave frequencies: A review [Wireless Corner]," *IEEE Antennas Propag. Mag.*, vol. 55, no. 4, pp. 262–287, Aug. 2013.

[23] "ANSYS HFSS—High frequency electromagnetic field simulation." [Online]. Available: http://www.ansys.com/Products/Electronics/ANSYS-HFSS, Accessed on: 27 Oct., 2016.

[24] T. S. Rappaport, *Wireless Communications: Principles and Practice*, vol. 2. Englewood Cliffs, NJ, Prentice-Hall, 1996.

[25] M. A. Stuchly, A. Kraszewski, S. S. Stuchly, and A. M. Smith, "Dielectric properties of animal tissues in vivo at radio and microwave frequencies: Comparison between species," *Phys. Med. Biol.*, vol. 27, no. 7, pp. 927–936, 1982.

[26] S. Gabriel, R. W. Lau, and C. Gabriel, "The dielectric properties of biological tissues: II. Measurements in the frequency range 10 Hz to 20 GHz," *Phys. Med. Biol.*, vol. 41, no. 11, pp. 2251–2269, 1996.

[27] A. Rahman and Y. Hao, "A novel tapered slot CPW-fed antenna for ultra-wideband applications and its on/off-body performance," in *Proc. 2007 Int. Workshop Antenna Technol.: Small Smart Antennas Metamaterials Appl.*, Mar. 2007, pp. 503–506.

[28] K. Y. Yazdandoost and K. Sayrafian-Pour, "Channel model for body area network (BAN)," Tech. Rep. IEEE P802, vol. 15, 2009.

[29] R. Chavez-Santiago *et al.*, "Propagation models for IEEE 802.15. 6 standardization of implant communication in body area networks," *IEEE Commun. Mag.*, vol. 51, no. 8, pp. 80–87, Aug. 2013.
[30] W. C. Y. Lee, *Mobile Cellular Telecommunications Systems*, 1st ed. New York, NY, USA: McGraw-Hill, Nov. 1988.

Ali Fatih Demir (S'08) received the B.S. degree in electrical engineering from Yildiz Technical University, Istanbul, Turkey, in 2011 and the M.S. degrees in electrical engineering and applied statistics from Syracuse University, Syracuse, NY, USA, in 2013. He is currently working toward the Ph.D. degree with the Wireless Communication and Signal Processing Group, Department of Electrical Engineering, University of South Florida, Tampa, FL, USA.

His current research interests include *in vivo* wireless communications, biomedical signal processing, and brain–computer interfaces.

Qammer H. Abbasi (S'08–M'12–SM'16) received the B.S. degree in electronics engineering from the University of Engineering and Technology, Lahore, Pakistan, in 2007, and the Ph.D. degree in electronic and electrical engineering from the Queen Mary University of London, London, U.K., in 2012.

He has been a Visiting Research Fellow with the Queen Mary University of London, since 2013. He joined the Department of Electrical and Computer Engineering, Texas A&M University at Qatar, Doha, Qatar, in August 2013, where he is currently an Assistant Research Scientist. His research interests include compact antenna design, radio propagation, body-centric wireless communications, cognitive/cooperative network, and multiple-input multiple-output systems.

Dr. Abbasi is a member of the Institution of Engineering and Technology.

Z. Esat Ankarali (S'15) received the B.S. degree in control engineering from Istanbul Technical University, Istanbul, Turkey, in 2011 and the M.S. degree in electrical engineering from the University of South Florida, Tampa, FL, USA, in 2013, where he is currently working toward the Ph.D. degree with the Wireless Communication and Signal Processing Group, Department of Electrical Engineering.

His current research interests include multicarrier systems, physical layer security, and *in vivo* wireless communications.

Akram Alomainy (S'04–M'07–SM'13) received the M.Eng. degree in communication engineering and the Ph.D. degree in electrical and electronic engineering from the Queen Mary University of London (QMUL), London, U.K., in 2003 and 2007, respectively.

He joined the School of Electronic Engineering and Computer Science, QMUL, in 2007, where he is currently an Associate Professor with the Antennas and Electromagnetics Research Group. His research interests include compact antenna design for wireless body area networks, radio propagation characterization, antenna interactions with human body, and advanced algorithms for intelligent antenna systems.

Dr. Alomainy is a member of the Institution of Engineering and Technology.

Khalid Qaraqe (M'97–SM'00) received the B.S. degree in electrical engineering (EE) from the University of Technology, Baghdad, Iraq, in 1986, the M.S. degree in EE from the University of Jordan, Amman, Jordan, in 1989, and the Ph.D. degree in EE from Texas A&M University, College Station, TX, USA, in 1997.

He joined the Department of Electrical and Computer Engineering, Texas A&M University at Qatar, Doha, Qatar in July 2004, where he is currently a Professor. His research interests include communication theory, mobile networks, cognitive radio, diversity techniques, and beyond fourth-generation systems.

Erchin Serpedin (S'96–M'99–SM'04–F'13) received the specialization degree in signal processing and transmission of information from Ecole Superieure D' Electricite, Paris, France, in 1992, the M.S. degree from the Georgia Institute of Technology, Atlanta, GA, USA, in 1992, and the Ph.D. degree in electrical engineering from the University of Virginia, Charlottesville, VA, USA, in January 1999.

He is a Professor with the Department of Electrical and Computer Engineering, Texas A&M University, College Station, TX, USA. His research interests include signal processing, biomedical engineering, and machine learning.

Prof. Serpedin is serving as an Associate Editor of the *IEEE Signal Processing Magazine* and as the Editor-in-Chief of *European Association for Signal Processing Journal on Bioinformatics and Systems Biology*.

Huseyin Arslan (S'95–M'98–SM'04–F'16) received the B.S. degree from Middle East Technical University, Ankara, Turkey, in 1992, and the M.S. and PhD. degrees from Southern Methodist University, Dallas, TX, USA, in 1994 and 1998, respectively.

From January 1998 to August 2002, he was with the research group of Ericsson Inc., Research Triangle Park, NC., USA, where he was involved with several projects related to 2G and 3G wireless communication systems. Since August 2002, he has been with the Department of Electrical Engineering, University of South Florida, Tampa, FL, USA, where he is currently a Professor. In December 2013, he joined Istanbul Medipol University, Istanbul, Turkey, where he has worked as the Dean of the School of Engineering and Natural Sciences. His current research interests include waveform design for 5G and beyond, physical layer security, dynamic spectrum access, cognitive radio, coexistence issues on heterogeneous networks, aeronautical (high altitude platform) communications, and *in vivo* channel modeling and system design.

Dr. Arslan is currently a member of the editorial board for the *Sensors Journal* and the IEEE SURVEYS AND TUTORIALS.